Journal of Physics: Conference Series **572** (2014) 012034 doi:10.1088/1742-6596/572/1/012034

The Influence of Carrier Dynamics on Double-State Lasing in Quantum Dot Lasers at Variable Temperature

V V Korenev[1], **A V Savelyev**[1], **A E Zhukov**[1,2], **A V Omelchenko**[1], **M V Maximov**[1,2]
[1]Saint–Petersburg Academic University RAS, Saint–Petersburg 194021, Russia
[2]Ioffe Physico–Technical Institute RAS, Saint–Petersburg 194021, Russia

E-mail: korenev@spbau.ru

Abstract. It is shown in analytical form that the carrier capture from the matrix as well as carrier dynamics in quantum dots plays an important role in double-state lasing phenomenon. In particular, the de-synchronization of hole and electron captures allows one to describe recently observed quenching of ground-state lasing, which takes place in quantum dot lasers operating in double-state lasing regime at high injection. From the other side, the detailed analysis of charge carrier dynamics in the single quantum dot enables one to describe the observed light-current characteristics and key temperature dependences.

1. Introduction

Efficient semiconductor lasers having broadband emission spectra, which correspond to the transparency window of standard silicon optical fibre and SiGe-waveguide, are required for a vast range of practical applications, from optical coherence tomography to ultrafast data transmission. It turns out that the emission spectrum of long-wavelength emitting InAs/InGaAs quantum dot (QD) lasers can overlap this practically useful wavelength range (*O-band*) even at room temperature and low injection current [1 – 3]. Moreover, the usage of these multi-frequency laser diodes for the optical data transmission is a promising alternative to currently used DFB-lasers (*distributed feedback lasers*) due to the simplicity and cheapness of their production [3].

At low injection and sufficiently low optical loss, the emission spectrum of InAs/InGaAs QD laser is formed by the ground state (GS) optical transitions of QDs emitting near 1.3 μm. Such a broadband emission is obtained owing to the involvement of different quantum dots into the lasing, having the different energies of ground-state optical transition due to the inhomogeneous broadening [5 – 8]. As the injection increases, the population of the excited energy levels (ES) of electrons and holes and, consequently, the population inversion of the ES optical transition of QDs, also tend to increase with injection [6]. As a result, at sufficiently high pump current the population inversion of ES reaches its threshold value and simultaneous GS- and ES-lasing, i.e., *double-state lasing*, takes place. Such a behaviour is confirmed by the series of experiments, which at sufficiently high injection revealed in the lasing spectra an additional spectral line (with $\lambda < 1.2$ μm) associated with the first excited-state (ES) optical transition of QDs [5 – 12]. Moreover, the usage of this simultaneous lasing via QD GS and ES optical transitions is the simplest way to obtain extremely broad emission spectrum in QD laser [3, 10 – 12]. The lasers operating in such a regime are also promising candidates for multi-wavelength optical networks pump and new laser sources [3, 9]. Therefore, the theoretical investigation of the double-state lasing phenomenon is the subject of interest in the current Paper.

2. Double-state lasing phenomenon

For the first time the double-state lasing phenomenon in InAs/InGaAs QD lasers was theoretically predicted by *Grundmann et al.* in [4] and then experimentally observed in [5 – 6], while its generally recognized explanation was proposed by *Markus et al.* in [6] and then developed in [7]. This approach is based on the system of rate equations for the QDs, which are described in terms of excitonic energy levels. At low injection and sufficiently low optical loss, GS-lasing takes place. As soon as the injection current is above GS-lasing threshold, the occupancy of GS excitonic energy level becomes fixed. However, the occupancy and, hence, the population inversion of the ES excitonic energy level of QD tends to increase with injection. As a result, at sufficiently high injection, double-state lasing takes place. After the onset of the double-state lasing, carrier population of both GS and ES energy levels remains unchanged. The flux of excitons from ES to GS level becomes limited by the finite relaxation time due to the well-known phonon-bottleneck effect [15]. Therefore, output power, which is emitted via GS optical transitions, reaches its maximal value and then stays constant for all injection currents exceeding the double-state lasing threshold [5 – 8]. Thereby, it is commonly implied that the onset of simultaneous GS- and ES-lasing leads to the stabilization of the GS-lasing power.

However, there are a number of experiments for InAs/InGaAs QD lasers, where the quenching or even complete damping of GS-lasing was observed as the injection is above double-state lasing threshold [10 – 14]. Light-current characteristics of 100-μm-wide and 4-mm-long laser sample having a single plane of MBE-grown InAs/InGaAs QDs are presented in the figure 1. As it can be seen from the figure, there is a definite contradiction between the predicted and real behaviour of QD laser.

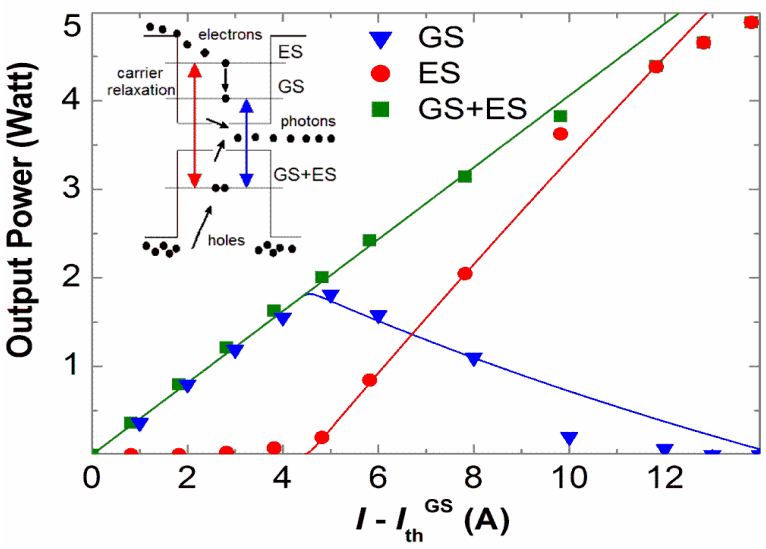

Figure 1. Experimental light-current characteristics (symbols) from [13] and their approximation (solid lines), where GS and ES correspond to the output power via GS and ES optical transitions of QDs, while GS+ES does to the total output power. Inset: QD energy levels diagram and optical transitions scheme.

To date, several attempts to explain the experimentally observed GS-lasing quenching were proposed. One of them is the self-heating of laser's active region operating in CW regime [10, 11]. If the self-heating effect takes place, with the increase of injection the red shift of lasing wavelength is expected to be observed in the experiments. However, as it was shown in [13] for the abovementioned samples, the increase of injection current from 5 to 12 A shifts the dominant laser emission peak only by 0.4 nm. This value corresponds to the increase of laser's active region temperature by only 1 ^{o}C and, in its turn, means that the self-heating effect cannot explain the observed GS-lasing quenching. Moreover, the experiments [13 – 14] show that the GS-lasing quenching occurs even in pulsed regime, when the self-heating is not pronounced.

At the same time, it was supposed in [12] that the increase of homogeneous broadening with the injection can lead to GS-lasing quenching due to the decrease of GS optical gain below the GS-lasing threshold. However, as it was shown in [13, 16], the dependence of homogeneous broadening on injection is not as strong as it was assumed in [12]. Thus, neither self-heating nor homogeneous broadening can completely describe the observed laser's behaviour in double-state lasing regime.

The more sophisticated models that do not imply both homogeneous broadening and self–heating effect are based on the assumption of the asymmetry in charge carrier distribution within a single QD [7, 14]. Indeed, the energy spacing between hole GS and ES energy levels is quite small (about 10 meV for typical InAs/InGaAs QDs [14]), hence an intensive exchange of carriers between these states takes place at room temperature so, that they can be considered as one effective hole reservoir – see the inset to figure 1. The "competition for the holes" between electrons occupying GS and ES levels takes place. Since the modal gain of the ES transition is approximately twice the gain of the GS transition, the ES-lasing line increases with pump at the expense of the GS one. To describe the observed GS-lasing quenching quantitatively authors of [14] had to introduce phenomenological linear emission rates of carriers from QD GS and ES into the matrix. This additional assumption seems to be artificial, since the authors did not verify it either by experiments or theoretical modelling.

It should be also noted that the complete quenching of GS-lasing in InAs/InGaAs QD lasers can be attributed to the growth of the internal loss with the increase of injection current as it was predicted in [17 – 18]. However, such a mechanism has to be accompanied by degradation of the laser's slope efficiency, which is not confirmed in the experiments – see figure 1. This, in its turn, means that the GS-lasing quenching cannot be described in the scopes of the assumption of the increase of internal loss and is determined by more subtle dynamic effects. Thus, the double-state lasing phenomenon and especially reasons for GS-lasing quenching still require an adequate theoretical description.

In order to explain the observed GS-lasing quenching we have recently proposed the new mechanism, which is based on the assumption of different hole and electron capture rates into QDs [19 – 20] and thereby takes into account the dynamics of charge carriers both in QDs and in matrix material. More precisely, we assume that the hole capture rate is lower than the electron one. The similar idea of de-synchronization between hole and electron captures was independently proposed in [16]. This assumption seems to be very natural, because the carrier capture rate is proportional to the velocity of their thermal motion in matrix material [21], while hole thermal velocity is lower than the electron one due to the higher effective mass of holes. The interplay between the difference in carrier capture rates and the aforementioned asymmetry [19 – 20] of their distribution in QD [14] intensifies the competition for the "common" holes between GS and ES electrons and, therefore, makes the process of depopulation of the effective hole level also more intensive. This, as a result, naturally accelerates the quenching of GS-lasing with the increase of injection.

To illustrate this qualitative understanding quantitatively, let us assume that each QD has only one hole and two electronic energy levels and there is no direct carrier exchange between the matrix and QD GS (see the inset to figure 1). Thus, neglecting the spontaneous recombination, one can obtain

$$\dot{f}_{e1} = \frac{D_2}{D_1}\cdot\left[g_{e21}\cdot f_{e2}\cdot\left(1-f_{e1}\right)-g_{e12}\cdot f_{e1}\cdot\left(1-f_{e2}\right)\right]-\frac{P_1}{D_1}, \tag{1}$$

$$\dot{f}_{e2} = g_{ec}\cdot\left(1-f_{e2}\right)-g_{ee}\cdot f_{e2}-g_{e21}\cdot f_{e2}\cdot\left(1-f_{e1}\right)+g_{e12}\cdot f_{e1}\cdot\left(1-f_{e2}\right)-\frac{P_2}{D_2}, \tag{2}$$

$$\dot{f}_{h} = g_{hc}\cdot\left(1-f_{h}\right)-g_{he}\cdot f_{h}-\frac{P_1+P_2}{D_1+D_2}. \tag{3}$$

Here, $P_{1(2)}$ is the rate of stimulated emission from QD GS(ES), $D_{1(2)}$ are the degrees of their degeneracy (for the common hole level the degeneracy is assumed to be D_1+D_2), $g_{e(h)c}$ and $g_{e(h)e}$ are the capture (into empty QD) and emission (from QD with one carrier) rates of an electron (hole), g_{e21} and g_{e12} are the rates of electron ES to GS and reverse transitions, $f_{e1(2)}$ and f_h are the occupancies of

electronic GS (ES) and effective hole energy levels. System (1) – (3) should be completed with the following conditions, which correspond to different lasing regimes

$$(NL):\ P_1 = 0,\ P_2 = 0, \tag{4}$$

$$(GS):\ \gamma_1 = f_{e1} + f_h - 1,\ P_2 = 0, \tag{5}$$

$$(GS + ES):\ \gamma_1 = f_{e1} + f_h - 1,\ \gamma_2 = f_{e2} + f_h - 1, \tag{6}$$

$$(ES):\ P_1 = 0,\ \gamma_2 = f_{e2} + f_h - 1, \tag{7}$$

$$\gamma_{1(2)} = \frac{\alpha_{in} + \alpha_{out}}{G_{\max 1(2)}}. \tag{8}$$

Here, $\gamma_{1(2)}$ is the population inversion required for GS(ES)-lasing that is defined in accord with Eq. (8), α_{in} and α_{out} are the internal and output losses, $G_{max1(2)}$ is the maximal gain of the GS(ES) optical transition. Eq. (4) corresponds to the regime of no lasing (*NL*), (5) does to pure GS-lasing (*GS*), (6) does to simultaneous GS- and ES-lasing (*GS+ES*), and (7) does to pure ES-lasing (*ES*). Taking into account conditions (4) – (8) one can obtain the stimulated emission rates via GS and ES (P_1 and P_2) optical transitions of QDs at any given electron and hole capture rate values (g_{ec} and g_{hc}) by solving system (1) – (8) numerically. Output power of GS and ES emission (W_1 and W_2) and the injection current (I) can be then calculated using well-known equations [22]

$$W_{1,2} = \frac{\alpha_{out}}{\alpha_{in} + \alpha_{out}} \cdot N_{QD} \cdot E_{1,2} \cdot P_{1,2},\ I - I_{th}^{GS} = \frac{N_{QD} \cdot e}{\eta_{id}} \cdot (P_1 + P_2), \tag{9}$$

where $E_{1(2)}$ is the energy of the GS(ES) optical transition, N_{QD} is the total number of QDs in the laser's active region, I_{th}^{GS} is the threshold current of GS-lasing, η_{id} is the internal differential quantum efficiency, and e is the charge of the electron. The η_{id} can be directly obtained from the experimental data presented in figure 1 and is equal to 61%.

For the detailed analysis of double-state lasing, it is convenient to introduce the h-factor ($h \equiv g_{hc}/g_{ec}$). As it was previously stated, we expect that $h < 1$. Assuming that h does not depend on the injection, one can calculate the dependence of GS-power as a function of injection current for different values of h, in order to show the influence of hole-to-electron capture rate ratio on GS-lasing – see figure 2. The other parameters are in accord with [13]: $g_{ee} = 219\ ns^{-1}$, $g_{he} = 19\ ns^{-1}$, $g_{e21} = 1250\ ns^{-1}$, $\alpha_{in} = 1.5\ cm^{-1}$, $\alpha_{out} = 3.1\ cm^{-1}$, $D_1 = 2$, $D_2 = 4$, $E_1 = 983$ meV, $E_2 = 1050$ meV, $G_{max1} = 6\ cm^{-1}$, $G_{max2} = 12\ cm^{-1}$.

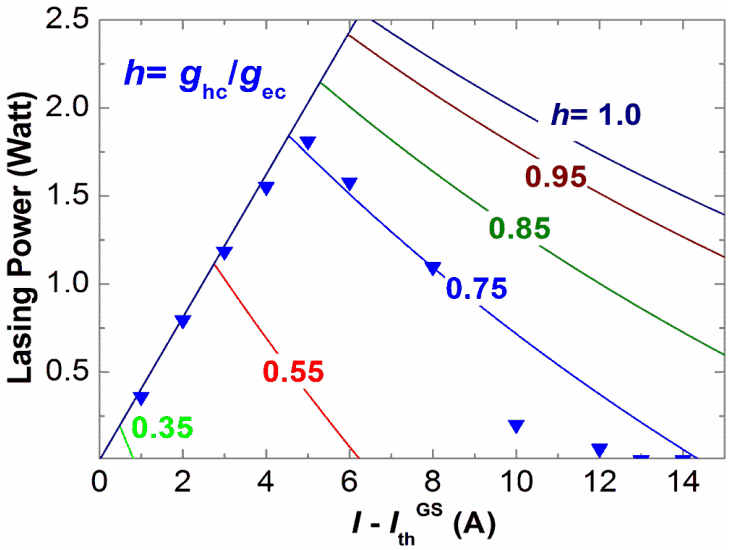

Figure 2. Light-current characteristics corresponding to GS-lasing component for different values of hole-to-electron capture rate ratio h (solid lines) and experimental data (symbols) from [13].

As it can be seen from the figure 2, even a small change of h (from unity to 0.75) leads to significant acceleration of GS-lasing damping and decrease of the maximum GS-lasing power by more than 40%. Therefore, we suppose that hole-to-electron capture rate ratio (h-factor) has a strong effect on the key lasing parameters. In particular, h can differ from the unity and should be taken into account to describe laser operation correctly. The best agreement between the proposed theory and the experimental data presented in the figure 1 is achieved for h= 0.75.

At the same time, the majority of works are based only on numerical analysis of the question that complicates the analysis and finding of key parameters, responsible for the double-state lasing. Therefore not only does numerical, but also analytical approach to this phenomenon is also important.

3. Analytical approach to the carrier dynamics in quantum dots

To solve the system of rate equations (1) – (9) analytically, it is convenient to introduce following dimensionless parameters

$$P_e = \frac{g_{ec}}{g_{ec}+g_{ee}},\ P_h = \frac{g_{hc}}{g_{hc}+g_{he}},\ P_{ve,vh} = 1 - P_{e,h},\ \widetilde{P}_{1,2} = \frac{P_{1,2}}{D^2\cdot\left(g_{ec}+g_{ee}\right)}, \tag{10}$$

$$D = \frac{D_2}{D_1},\ C = \left(\frac{1}{1+D^{-1}}\right)\cdot\frac{g_{ec}+g_{ee}}{g_{hc}+g_{he}},\ \eta = \frac{g_{ec}+g_{ee}}{g_{e21}},\ \xi = \frac{g_{e12}}{g_{e21}}. \tag{11}$$

In terms of introduced parameters the solution of the system (1) – (9) can be obtained in analytical form at any given electron and hole capture rates (g_{ec} and g_{hc}) in all possible lasing regimes

A) <u>*NL*–regime</u>: $$\widetilde{P}_1 = \widetilde{P}_2 = 0,\ f_{e1} = \frac{P_e}{\left(1-\xi\right)\cdot P_e + \xi},\ f_{e2} = P_e,\ f_h = P_h, \tag{12}$$

where ξ= exp[$(E_1 - E_2)/T$], T is laser's temperature in meV; ξ is an order of 0.1 at room temperature.

B) <u>*GS*–regime</u>:

$$\left[C\cdot\left(1-\xi\right)\right]\cdot\widetilde{P}_1^2 + \left[\left(1-\xi\right)\cdot\gamma_1 - \eta - C\cdot\left(P_e+\xi\cdot P_{ve}\right) - \left(P_h+\xi\cdot P_{vh}\right)\right]\cdot\widetilde{P}_1 + \ldots$$
$$\ldots + \left[\left(P_e\cdot P_h - \xi\cdot P_{ve}\cdot P_{vh}\right) - \gamma_1\cdot\left(P_e+\xi\cdot P_{ve}\right)\right] = 0,\ \widetilde{P}_2 = 0, \tag{13}$$

$$f_{e1} = \frac{\left(1+\eta\right)\cdot\widetilde{P}_1 - P_e}{\left(\xi-1\right)\cdot\left(P_e-\widetilde{P}_1\right) - \xi},\ f_{e2} = P_e - \widetilde{P}_1,\ f_h = P_h - C\cdot\widetilde{P}_1, \tag{14}$$

where result for $\widetilde{P}_1$ is presented in the form square equation for brevity (minor root should be used). In GS-regime the population inversion of QD GS is fixed.

C) <u>(*GS*+*ES*)–regime</u>: $$\widetilde{P}_1 = \frac{f_{e2}\cdot\left(1-f_{e1}\right) - \xi\cdot f_{e1}\cdot\left(1-f_{e2}\right)}{\eta},\ \widetilde{P}_2 = \frac{P_h - f_h}{C} - \widetilde{P}_1, \tag{15}$$

$$f_{e1,2} = 1 + \gamma_{1,2} - f_h,\ f_h = P_h - \frac{C\cdot\left[P_e + P_h - 1 - \gamma_2\right]}{C+1}. \tag{16}$$

In the case of (GS+ES)-regime, population inversion of both GS and ES optical transitions are fixed.

D) <u>*ES*–regime</u>: $$\widetilde{P}_1 = 0,\ \widetilde{P}_2 = \frac{P_h - f_h}{C}, \tag{17}$$

$$f_{e1} = \frac{f_{e2}}{f_{e2}\cdot\left(1-\xi\right)+\xi},\ f_{e2} = \frac{C\cdot P_e - P_h + 1 + \gamma_2}{C+1},\ f_h = 1 + \gamma_2 - f_{e2}. \tag{18}$$

Finally, when stimulated emission comes from the ES only, the population inversion of only ES persists equal to constant.

Moreover, using (10) – (18) it is possible to provide analytical conditions separating different regimes of laser emission and, therefore, to find out corresponding lasing regime for any given pair (g_{ec}, g_{hc}). This allows one to predict, when the switching between the regimes takes place. Thus, at

sufficiently low injection corresponding to low values of g_{ec} and g_{hc}, both population and population inversion of GS and ES are sufficiently small, there is no stimulated emission can be seen

$$\begin{cases} \dfrac{P_e}{P_e \cdot (1-\xi)+\xi} + P_h - 1 < \gamma_1 \\ P_e + P_h - 1 < \gamma_2 \end{cases}. \quad (19)$$

Pure GS-lasing takes place at higher injection, when the population inversion between hole and electron GS of QD reaches its threshold value, while the population of electronic ES and, consequently, the population inversion of ES optical transition, stays still below corresponding lasing threshold so, that there is no ES-lasing. This corresponds to the following condition

$$(C+1)\cdot f_{e2} - C \cdot P_e + P_h - 1 < \gamma_2, \quad (20)$$

where f_{e2} is in accord with (14).

In order to reach the conditions of double-state lasing regime, the population inversion of ES ($f_{e2} + f_h - 1$) should become high enough for ES-lasing, while the population inversion of GS ($f_{e1} + f_h - 1$) should be still high enough in order to maintain GS-lasing. Therefore, simultaneous GS- and ES-lasing takes place, if the two following conditions are fulfilled

$$f_{e2} + f_h - 1 > \gamma_2, \quad (21)$$

where the values, used for f_{e2} and f_h are defined by (13) – (14), and the condition

$$f_{e1} + f_h - 1 > \gamma_1, \quad (22)$$

where the values, used for f_{e1} and f_h are in accord with (18).

After the onset of double-state lasing the population of electronic GS tends to decrease, and at sufficiently high injection the population inversion of GS optical transition drops below the threshold of GS-lasing. In this case pure ES-lasing regime takes place that corresponds to following condition

$$f_{e1} + f_h - 1 < \gamma_1, \quad (23)$$

where the values, which should be used for f_{e1} and f_h, are in accord with (18).

Within the framework of the discussion above (in the end of *Section 2*), it is possible to consider the question of separation between different lasing regimes in terms of hole-to-electron capture rate ratio (h). It should be emphasized that there is two critical values of h: h_{cr} and h^*. If $h > h_{cr}$ ($h_{cr} \sim 0.9$ for the parameters used), there is no GS-lasing quenching can be seen, however if $h < h_{cr}$, the complete quenching of GS-lasing early or later takes place depending on the value of h. Finally, if h is low enough ($h < h^* \sim 0.17$ for the parameters used), there is no GS-lasing seen at all. The expressions for h_{cr} and h^* can be obtained from Eqs. (1) – (8) in analytical form

$$h_{cr} = \frac{2}{3}\cdot\frac{t}{1-t-\gamma_2},\ h^* = \frac{g^*_{hc}}{g^*_{ec}},\ g^*_{ec} = g_{ee}\cdot\frac{1-t}{t},\ g^*_{hc} = g_{he}\cdot\frac{t+\gamma_2}{1-t-\gamma_2}, \quad (24)$$

where parameter t is given by the following equation

$$t^2 - (\gamma_1 - \gamma_2 + 1)\cdot t + (\gamma_1 - \gamma_2)\cdot g_{e21}/(g_{e21} - g_{e12}) = 0. \quad (25)$$

It can be also shown that the increase of output loss (decrease of the sample length) results in the increase of h_{cr} value. As a result, the range of the h-factor values, where GS-lasing can occur, becomes narrower up to complete shrinkage at sufficiently high loss.

4. Temperature dependence of threshold currents

It turns out that in terms of the proposed model it is also possible to describe the temperature dependences of threshold current densities of double-state lasing (j_{th}^{ES}) and complete quenching of the GS-lasing (j_{off}^{GS}) qualitatively and quantitatively, see figure 3.

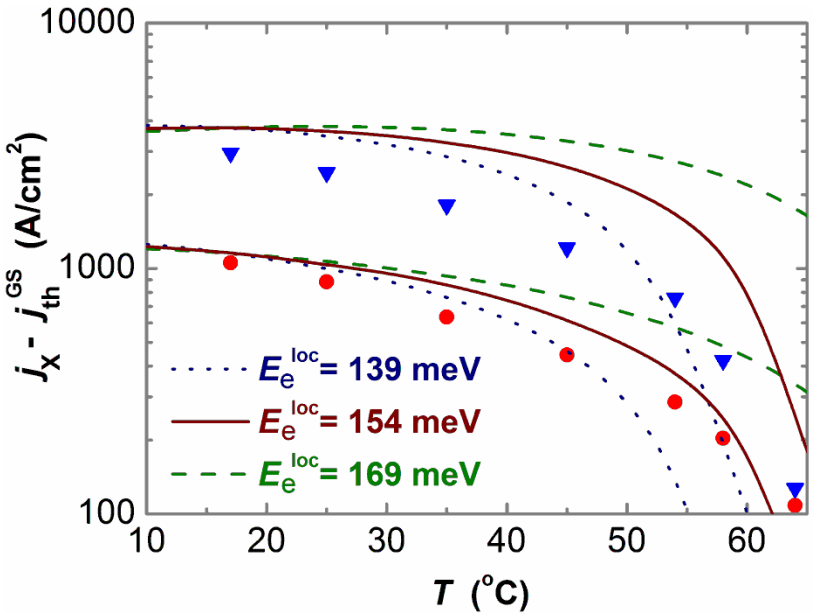

Figure 3. Experimental temperature dependence of threshold current density of double-state lasing (red circles) and complete quenching of GS-lasing (blue triangles), while the lines correspond to calculation.

We used in calculation the same set of parameters as for figure 1, in particular the value of h is assumed to be 0.75, whereas the localization energy of electrons (E_e^{loc}) is varied in the range from 139 to 169 meV. Taking into account that the ES-lasing line is 1.18 μm, the bandgap of GaAs is 0.870 μm and the asymmetry in hole and electron localization energies [23], one can calculate the temperature dependence of the threshold current densities. As it can be seen from the figure 3, the best agreement between the experimental data and its theoretical approximation is achieved for E_e^{loc}= 154 meV that is in accord with real experiment [23]. The fact that the parameters' values used for calculation of all figures 1 – 3 correspond to the real experiment also proves the proposed model of double-state lasing.

The decrease of both characteristic current densities with the temperature, which is seen from the figure 3, can be explained by the decrease of the ES-to-GS ($g_{e21}\cdot f_{e2}\cdot[1-f_{e1}]$) and the increase of the GS-to-ES ($g_{e12}\cdot f_{e1}\cdot[1-f_{e2}]$) electron transition rate at fixed injection. Thus, in double-state lasing regime the increase of the temperature leads to the decrease of the effective flux of carriers coming to the electron GS that, in its turn, is proportional to the output power via GS optical transition of QDs – see Eq. (1). Therefore, the GS-lasing power also tends to decrease with the increase of the temperature that ultimately leads to the complete damping of GS-lasing at sufficiently high temperature.

5. Conclusion

As a result, the influence of charge carrier dynamics on output power of QD laser operating in double-state lasing regime was studied analytically. Under the assumption of different hole and electron capture rates in QDs, the mechanism of GS-lasing quenching was proposed. The analytical conditions describing switching between different lasing regimes at variable injection were obtained. Temperature dependences of key threshold currents were also considered. It was figured out that only the simultaneous consideration of charge carrier dynamics in matrix and in quantum dots allows one to describe the observed temperature dependences, as well as ground-state lasing quenching, correctly.

Acknowledgements

This work was supported by the Program of Fundamental Research of Russian Academy of Sciences, Russian Foundation for Basic Research, by Federal Program "Scientific and scientific-pedagogical personnel of innovative Russia" of the Ministry of Education and Science of the Russian Federation and by the Dynasty Foundation.

References

[1] Zhukov A E and Kovsh A R 2008 *Quantum Electronics* **38** 409
[2] Zhukov A E, Kovsh A R, Nikitina E V, Ustinov V M, Alferov Zh I 2007 *Semicond.* **41** 606
[3] Djie H S, Ooi B S, Fang X, Wu Y, Fastenau J M, Liu W K, Hopkinson M 2007 *Opt. Lett.* **32** 44
[4] Grundmann M, Weber A, Goede K, Ustinov V M, Zhukov A E, Ledentsov N N, Kop'ev P S, Alferov Zh I 2000 *Appl. Phys. Lett.* **77** 4
[5] Zhukov A E, Kovsh A R, Livshits D A, Ustinov V M, Alferov Zh I 2003 *Semic. Sci. Tech.* **18** 774
[6] Markus A and Fiore A 2004 *Phys. Stat. Sol.* (a) **201** 338
[7] Shi L W, Chen Y H, Xu B, Wang Z C, Wang Z G 2007 *Physica E* **39** 203
[8] Jiang L and Asryan L V 2006 *IEEE Phot. Tech. Lett.* **18** 2611
[9] Naderi N A, Grillot F, Yang K, Wright J B, Gin A, Lester L F 2010 *Opt. Express* **18** 27028
[10] Kim Y J, Joshi Y K and Fedorov A G 2010 *J. Appl. Phys.* **107** 073104
[11] Ji H M, Yang T, Cao Y L, Xu P F, Gu Y X, Wang Z G 2010 *Jpn. J. Appl. Phys.* **49** 072103
[12] Sugawara M, Hatori N, Ebe H, Ishida M, Arakawa Y, Akiyama K, Otsubo T and Nakata Y 2005 *J. Appl. Phys.* **97** 043523
[13] Zhukov A E, Maximov M V, Shernyakov Yu M, Livshits D A, Savelyev A V, Zubov F I, Klimenko V V 2012 *Semicond.* **46** 231
[14] Viktorov E A, Mandel P, Tanguy Y, Houlihan J, Huyet G 2005 *Appl. Phys. Lett.* **87** 053113
[15] Sugawara M, Mukai K, Shoji H 1997 *Appl. Phys. Lett.* **71** 2791
[16] Gioannini M 2012 *J. Appl. Phys.* **111** 043108
[17] Asryan L V, Luryi S 2003 *Appl. Phys. Lett.* **83** 5368.
[18] Zhukov A E, Kovsh A R, Ustinov V M, Alferov Zh I 2003 *Laser Phys.***13** 39.
[19] Korenev V V, Savelyev A V, Zhukov A E, Omelchenko A V, Maximov M V 2013 *Appl. Phys. Lett.* **102** 112101
[20] Korenev V V, Savelyev A V, Zhukov A E, Omelchenko A V, Maximov M V, Shernyakov Yu M 2012 *Proc. of SPIE* **8432** 84321L
[21] Asryan L V and Suris R A 1996 *Semicond. Sci. Technol.* **11** 554
[22] Agrawal G P, Dutta N K 1993 *Semiconductor Lasers* New York (Van Nostrand Reinhold) 58
[23] Höglund L, Karlsson K F, Holtz P O, Pettersson H, Pistol M E, 2010 *Phys. Rev.* B **82** 035314